LES OF SOOTING FLAMES

Grant/Contact Number: DAAD19-03-1-0049
Principal Investigator: Suresh Menon

School of Aerospace Engineering
Georgia Institute of Technology, Atlanta, GA 30332

SUMMARY/OVERVIEW

Prediction of soot formation in turbulent flames is a major challenge due to the chemical complexity and the barely understood coupling between soot formation and the other flow transient processes. The current objective is to develop a unified, general methodology for large-eddy simulation (LES) of soot formation and transport in turbulent flames.

TECHNICAL DISCUSSION

A subgrid model for soot dynamics is developed for LES, which uses the method of moment approach with Lagrangian Interpolative closure (MOMIC) so that no a priori knowledge of the particle distribution is required. The non-coalescent limit, as well as the soot transport by diffusion and thermophoretic forces is included. The soot model is implemented within a subgrid mixing and combustion model based on the linear-eddy mixing (LEM) model so that gas phase reaction-diffusion and soot related MOMIC coupling is implemented without ad hoc filtering. Relatively detailed multi-species ethylene-air kinetics mechanism [1] is employed for gas phase combustion, and is combined with a four-step soot formation model. The LES model is used to study the effect of turbulence and the C/O ratio effect on soot production in a turbulent premixed flames in the thin reaction zone regime. In addition, a study is conducted to evaluate the effect of using a constant versus variable transport properties for the gas phase species. Finally, two non-premixed cases, sooting and non-sooting are compared with experiment to validate the model.

The general methodology of the subgrid model is shown in Fig. [1]. The soot nucleus is assumed to be composed of two carbon atoms. Acetylene is decomposed to give a soot nucleus and hydrogen dioxide around 1000 K as shown in Fig. [2]. Soot nuclei collide together to coalesce and give larger soot particles. During which, oxidative attack of oxygen and hydroxyl continue to decay the soot surface and reduce the soot particle mass by oxidizing carbon atoms to carbon monoxide and hydrogen radicals. After a transient period the soot particle diameter exceed a certain threshold, after which coalescent collision is not physical anymore and the soot particles start to agglomerate. These processes are coupled with soot diffusion, gas phase chemistry and thermphoretic transport due to temperature gradients. The thermophoretic forces and soot diffusion has been implemented based on a recent generalized study that satisfy the specular as well as the diffuse collision limits in the free molecular regime [2].

(a) LES of Turbulent Premixed Ethylene Flames

Earlier studies [3] addressed the effect of C/O ratio and turbulence on soot formation in a turbulent premixed flame. Two studies have also been conducted to compare the effect of using detailed variable binary diffusion coefficients [1]. Since, the critical C/O ratio for soot formation in ethylene/air premixed flames is around 0.6, the C/O ratio for both cases is 0.677. The test conditions for these cases are summarized in Table [1]. The grid resolution is a 64x64x64 cube

of a domain of 1.5x1.5x1.5 mm, with 12 LEM cells. The LEM resolution is chosen to capture the flame thickness and to resolve close to the Kolomogorov length scale (1-2 η).

The turbulent flame is highly strained and the curvature effect changes the species profiles according to the ratio of the thermal to the molecular diffusivity. The flame stretch is induced by the flow non-uniformity (strain effect) and the curvature due to the wrinkling of the flame surface area, which increases its reaction front. When the flame has negative curvature (concave towards the reactants) the mass is focused towards the products side, and the heat is focused inwards to the reactants side. If the Lewis number (Le) is greater than unity, the thermal diffusivity will increase the temperature in the preheat zone and the flame burns strongly with a higher flame temperature. These observations are confirmed in Fig. [3], where the C_2H_4 reaction rate and temperature profile across a concave and a convex flame elements are plotted. The flame shows higher temperature and reaction rate across the concave element. Figure [4] shows the PDF of mean curvature for both test cases. The figure shows that the constant diffusion flame is skewed towards the positive curvature (convex towards reactants), while the variable diffusion case is more symmetric with higher probabilities in the negative curvature side. The wide range of curvature indicates the turbulence effect on the flame structure and the surface area. In addition, the variable diffusivity case shows wider tails and no sharp peaks in the middle. The wider tails indicates the presence of more flames close to the spherical and saddle shapes. The mean in both cases is around zero. The variable diffusion case predicts higher peak value of the soot volume fraction. However, the constant diffusivity case shows a slightly wider profile for the temperature and the soot volume fraction. The wider profile is a direct consequence of the higher Le (higher thermal diffusivity). The higher soot production is a direct result of the higher surface growth rate. Figure [5] shows that the higher relative thermal to molecular diffusivity in the constant diffusion coefficients increases the collision frequency and the coagulation rate and that in turn reduces the number density and the soot surface growth rate.

(b) LES of Turbulent Premixed Flames

The eventual goal of the current development is to study soot formation in realistic turbulent non-premixed flames of practical interest. As a precursor to this goal, two studies are conducted for a non-premixed hydrocarbon flame. A non-sooting methane swirling, bluff body stabilized flame is used for initial validation. Figures [6] show the centerline mean axial velocity component for three simulated experimental flames [3]. The centerline shows existence of a centerline recirculation bubble for the SM1 flame. The rate of decay of the central jet is captured reasonably using the LEMLES approach. The flame and flow structure visualization is shown in Figs [7, 8] for the SM1 and SMA2 flames, respectively. More discussion are given elsewhere [5]. A base recirculation zone RZ is established for the SM1 flame in addition to a centerline recirculation bubble VBB. In-between the base RZ and the swirl-induced VBB, there exists a collar-like vertical shear region with high rotational (azimuthal) velocity as the separated shear layer first turns towards the centerline and then diverges around the VBB. The contour plots of constant mean ϕ are superimposed to show the flame structure. The black boundary is the stoichiometric line. In comparison, the SMA2 flame shows only a single elongated RZ downstream of the bluff body and no VBB is observed due to the higher fuel jet axial velocity.

The case is a sooting ethylene jet flame [6]. This study is still underway. Figure [9] shows the iso-surface for the axial velocity component. The jet spread rate grows roughly linear with the axial distance, which is consistent with the classical results for the axisymmetric turbulent jet. Figure [10] shows the flame structure on a median cross section and the soot mass fraction contours. The flame is slightly lifted, which is similar to the experimental results, soot is formed at the centerline far downstream. More details will be reported soon.

SUMMARY and FUTURE PLANS

The soot validation jet case will be continued to compare with the experimental jet results. The effect of coagulation and soot diffusion, thermophoresis and agglomeration is all under current investigation as well. Finally, the soot model will be connected to a Lagrangian approach to track the soot particles formation and destruction history.

Flame	C/O	Re	Da	Ka	S_L(m/sec)	δ_F	u'	l(mm)	u'/S_L	l/δ_F	η(mm)
F1	0.67	271	1.15	23.76	0.24	0.11	2.86	1.47	11.9	13.71	0.02

Table [1]

REFERENCES

[1] T.F. Lu and C.K. Law, *Proc. Combust. Inst.*, 30 (1) (2005) 1333-1341

[2] Zhigang Li and Hai Wang, Physical Review E, 70, 021205 (2005)

[3] http://www.aeromech.usyd.edu.au/thermofluids/switl.html, University of Sydney, 2005

[4] H. El-Asrag, S. Menon, AIAA-2006-153, 2006.

[5] H. El-Asrag, S. Menon, *Proc. Combust. Inst.*, accepted, 2006

[6] B. Yang, U. Koylu, Combust. Flame, 144 (2005) 55-65

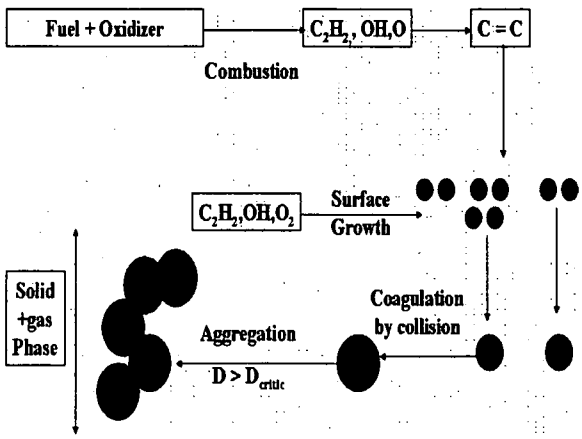

Figure 1 Soot model components

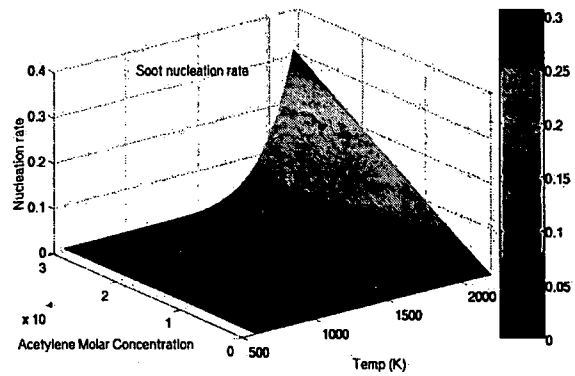

Figure 1 Nucleation rate (vertical axis) variation with temperature and acetylene molar fraction

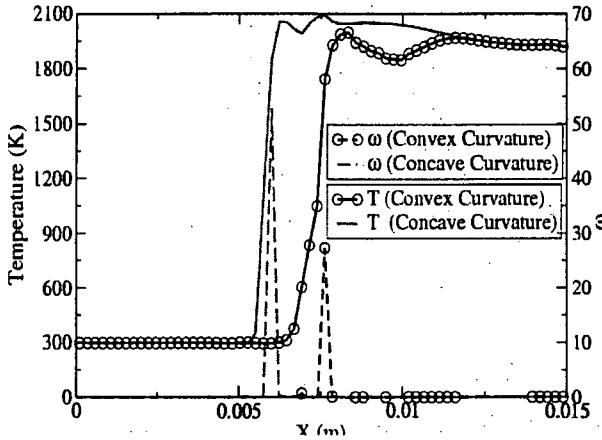

Figure 2 Temperature and ethylene reaction rate at a concave and convex flame segments with variable diffusion coefficients

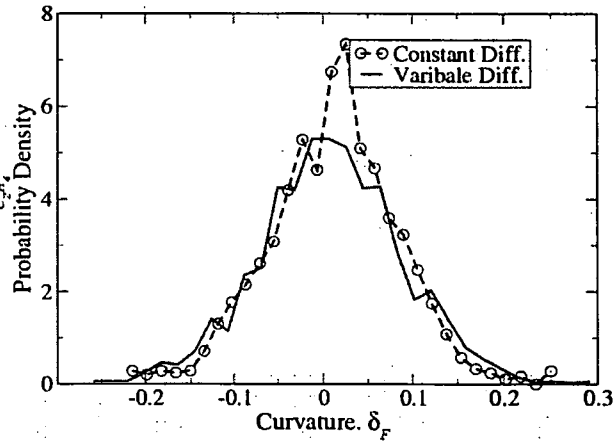

Figure 3 Mean Curvature probability density function (PDF)

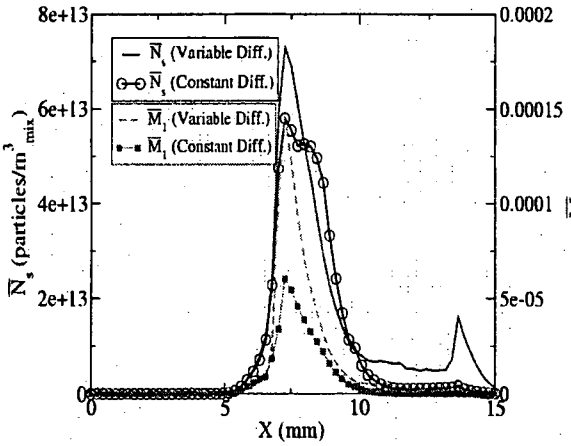

Figure 5 Mean soot number density (left) and average mass per unit volume (right)

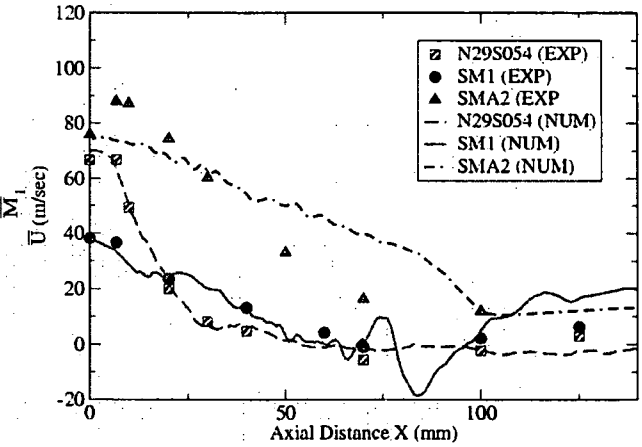

Figure 4 Centerline variation of time averaged axial velocity

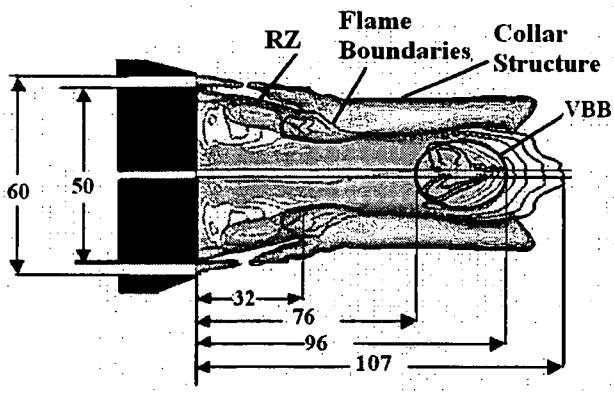

Figure 6 SM1 flame flow field and flame structure

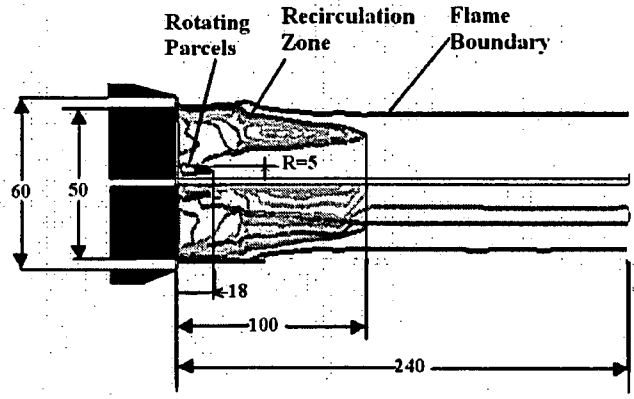

Figure 8 SMA2 flame flow field and flame structure

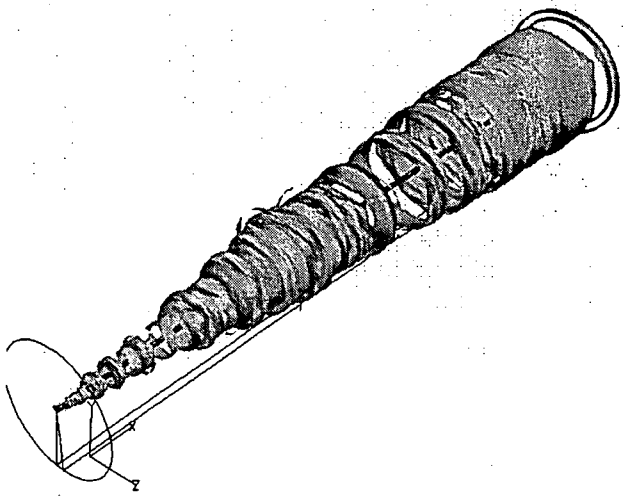

Figure 8 Axial velocity iso-surface

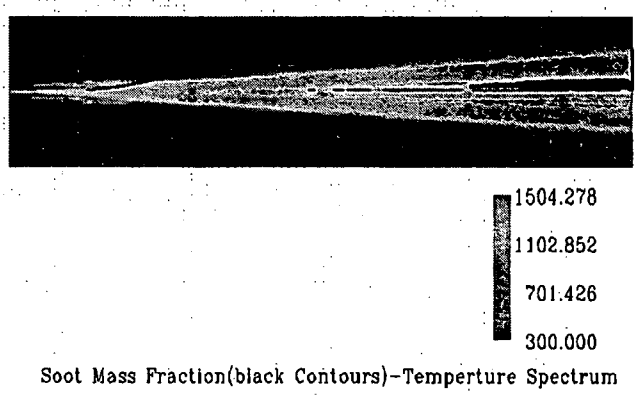

Figure 7 Temperature (spectrum) and soot contours